

Original Article

Statistical modeling of diffusive CO₂ emissions before the creation of the SINOP hydroelectric reservoir, Brazil

Modelagem estatística das emissões difusivas de CO₂ antes da formação do reservatório da usina hidrelétrica de SINOP, Brasil

J. P. P. Dias^{a*}  and M. A. Santos^b 

^aUniversidade Federal do Rio de Janeiro – UFRJ, Instituto Alberto Luiz Coimbra de Pós-graduação e Pesquisa de Engenharia – COPPE, Programa de Planejamento Energético – PPE, Rio de Janeiro, RJ, Brasil

^bUniversidade Federal do Rio de Janeiro – UFRJ, Laboratório de Energias Renováveis e Estudos Ambientais – LEREA, Rio de Janeiro, RJ, Brasil

Abstract

Several discussions have arisen about energy from hydroelectric plants being considered clean energy and its reservoirs have been investigated due to the large emission of greenhouse gases (GHG), such as carbon dioxide, methane, and nitrous oxide. The present work shows a statistical study of the diffusive CO₂ emissions before the formation of the reservoir of the hydroelectric power plant (HPP) of SINOP, Brazil. The association between emissions collected at the surface (water-air) and at the bottom of the reservoir (sediment-water) was investigated during four data collection campaigns, carried out from November 2017 to September 2018. This study aims to compare the effect of reservoir depth on the diffusive flow of CO₂ at 34 collection points. The variable depth analyzed was defined from points collected on the surface and bottom of the reservoir. The objective is to detect whether different periods of time and whether the depth of the reservoir have a direct impact on the behavior of diffusive CO₂ emissions. As the measurements of the observational unit are repeatedly observed, there is a multilevel structure, individuals are independent of each other, but there is an intra-individual correlation. Considering this data configuration, an estimation of generalized equations (GEE) was performed, which is a technique that estimates the intra-individual correlation matrix and thus produces estimates for the parameters of the generalized regression models (Generalized Regression Models – GLM) that are not biased. The study showed that the average diffusive CO₂ emissions are higher on the reservoir surface. The study also found that, on average, there are more emissions during the rainy season in the region than during the dry season.

Keywords: repeated measures, carbon dioxide, generalized estimation equations, greenhouse gases.

Resumo

Diversas discussões têm surgido a respeito da energia proveniente de usinas hidrelétricas ser considerada uma energia limpa e seus reservatórios têm sido investigados devido à grande emissão de gases de efeito estufa (GEE), como dióxido de carbono, metano e óxido nitroso. O presente trabalho traz um estudo estatístico das emissões difusivas de CO₂ antes da formação do reservatório da usina hidrelétrica (UHE) de SINOP, Brasil. Investigou-se a associação entre as emissões coletadas na superfície (água-ar) e no fundo do reservatório (sedimento-água) durante quatro campanhas de coletas de dados, realizadas no período de novembro de 2017 até setembro de 2018. Este estudo visa comparar o efeito da profundidade do reservatório no fluxo difusivo de CO₂ em 34 pontos de coleta. A variável profundidade analisada foi definida a partir de pontos coletados na superfície e no fundo do reservatório. O objetivo é detectar se épocas de tempo diferentes e se a profundidade do reservatório tem impacto direto no comportamento das emissões difusivas de CO₂. Como as medidas da unidade observacional são observadas repetidamente, tem-se uma estrutura multivariável, os indivíduos são independentes entre si, porém existe uma correlação intra-individuais. Considerando essa configuração de dados, foi feita uma estimativa de equações generalizadas (Generalized Estimating Equations – GEE) que é uma técnica que estima a matriz de correlação intra-individuos e assim, produz estimativas para os parâmetros dos modelos de regressão generalizados (Generalized Regression Models – GLM) que não sejam enviesadas. O estudo mostrou que as médias das emissões difusivas de CO₂ são maiores na superfície do reservatório. O estudo também detectou que em média, existem mais emissões durante o período de chuva na região do que durante a época da estiagem.

Palavras-chave: medidas repetidas, dióxido de carbono, equações de estimação generalizadas, gases de efeito estufa.

*e-mail: juliana.pereira@ppe.ufrj.br

Received: August 15, 2021 – Accepted: March 1, 2022



This is an Open Access article distributed under the terms of the Creative Commons Attribution License, which permits unrestricted use, distribution, and reproduction in any medium, provided the original work is properly cited.

1. Introduction

Hydroelectric plants play a fundamental role in supplying electricity in Brazil and around the world (Barbosa et al., 2018). The Brazilian electricity sector has a large base of large hydroelectric plants, 63.8% (government of Brasil, 2020), in addition to other sources of energy production, and transmission lines of continental dimensions, of varying voltage levels and technologies.

Brazilian hydroelectric plants have already been investigated for their contribution to the intensification of the greenhouse effect. Its reservoirs would be emitting greenhouse gas (GHG) such as methane (CH_4), carbon dioxide (CO_2) and nitrous oxide (N_2O) that would be produced through the decomposition of organic material in its accumulation basin (Mercado Burciaga et al., 2019; Damazio et al., 2013).

In many practical situations, there is an interest in modeling the behavior of one or more response variables measured in the units of one or more populations along some ordered dimension (Chen et al., 2018). In this study, the variable to be modeled is the CO_2 concentration along the Teles Pires river and the respective diffusive fluxes to the atmosphere, collected repeatedly over time.

The expression “repeated measures” is used to specify multiple observations of the same characteristic in one or more variable responses in the same experimental unit (Nobre and Singer, 2007).

Experiments with repeated measures over time involve two factors: treatments and time and are frequent in several areas of knowledge. The main purpose of this type of experiment is to examine and compare treatment trends over time. This may involve comparisons between treatments within each time, or comparisons of times within each treatment. Thus, treatment is the factor between individuals (experimental units) and time the factor between individuals.

In statistical science, when you have two or more observations, made at different times, of the response variable in each sample unit under investigation, this study is known as a longitudinal study that generates longitudinal data.

For many years, normal linear models have been used to describe most random phenomena. Even when the phenomenon under study did not present an answer to which the assumption of normality was reasonable, transformation was suggested to achieve normality.

With computational development, Nelder and Wedderburn (1972), proposed generalized linear models (MLGs). The basic idea was to open the range of options for the distribution of the response variable and give greater flexibility to the relationship between the average of the response variable and the linear predictor.

When the response variable is observed over time, there may be a correlation between the observations, and this may lead to a violation of independence. One way to consider the correlated data is to model the correlation structure, using the generalized estimation equation (GEE) approach, given by Liang and Zeger (1986).

In this work, a GHG model will be built with carbon dioxide as the response variable and depth and campaign

independent variables, to identify an effect of reservoir depth and time on diffusive CO_2 emissions. So, it must be that the points are the experimental units, the depth of the treatment and the campaigns the intra-individual factor.

In this sense, this work aims to apply statistical tools that can explain the behavior of diffuse carbon dioxide emissions in the Teles Pires river before the formation of the UHE SINOP reservoir.

2. Materials and Methods

2.1. Study area

The present study was carried out in the Teles Pires River before the construction of the hydroelectric power plant (HPP) SINOP reservoir, located in the state of Mato Grosso, Brazil. The reservoir has a direct influence on the municipalities of Itáubá/MT, Cláudia/MT, Ipiranga do Norte/MT, Sinop/MT and Sorriso/MT (Figure 1).

This plant has an installed capacity of 408 MW, with a powerhouse with two Kaplan-type turbines of 204 MW each. The maps generated with the values of each analyzed point were generated from the free software QGIS (Sherman et al., 2011).

The Teles Pires river basin has an area of approximately 150,000 km² and includes part of the territories of Mato Grosso and Pará.

The source of the Teles Pires River is in Serra Azul, in the municipality of Primavera do Leste, at an altitude of 800 meters. Its waters bathe two important Brazilian biomes: the Cerrado and the Amazon rainforest.

2.2. Diffusive water-air flow

Molecular diffusion is the part of transporting a solute in a fluid due solely to the agitation of the molecules that make up the fluid (Golbi, 2015). Diffusive flows depend on the concentration gradient between the micro surface layer and atmospheric and physical parameters such as wind speed and rain (Borges et al., 2004; Guérin et al., 2007).

The flow is calculated from the difference in gas concentration in ambient air inside a floating chamber on the water surface over a period (Abril et al., 2005). This flow depends on the difference in concentration in the ambient air and on the concentration in the water layer close to the surface, as well as on the speed of the winds and intensity of precipitation (IHA, 2010).

The diffusive flow of CO_2 represents the exchange of a chemical species from the diffusive molecular transport or turbulent diffusive transport between two phases or in the same phase. In the case of hydroelectric reservoirs, the flow between two phases is determined: aquatic and gaseous (when this flow is measured on aquatic surfaces).

For this study, the flow was measured by means of diffusion chambers, a method with greater use in international studies. The chamber holds a known volume of air trapped on the water surface that can receive gases that emanate from the water-air interface or leave this headspace for water (Figure 2).

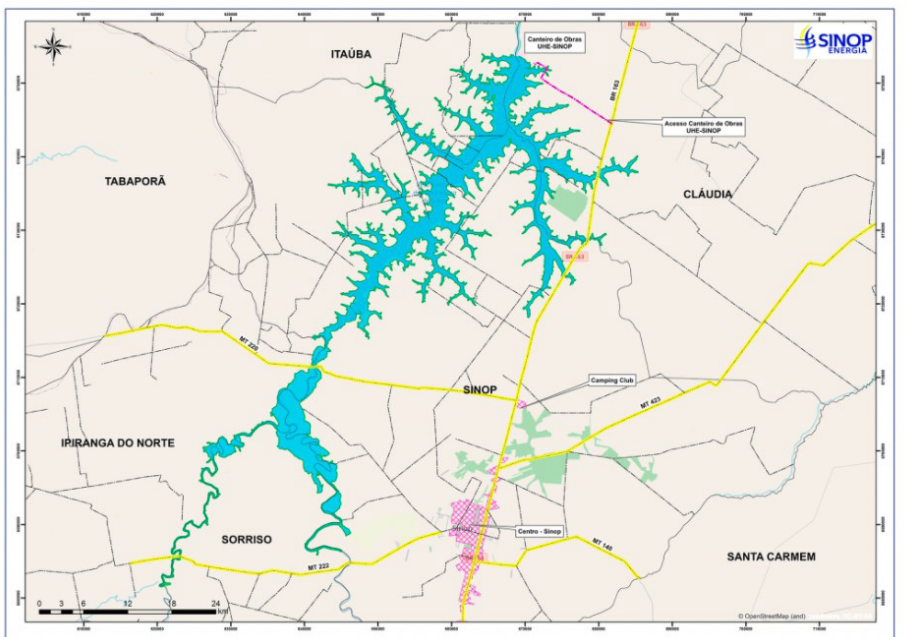


Figure 1. Location of the SINOP hydroelectric reservoir. Source: SINOP Energia (2021).



Figure 2. Diffusion gas collecting chamber showing protective shield against bubbles. Source: COPPE (2018).

2.3. Sediment-water diffusive flow

The sediments were collected with the aid of a Kajak-Brinkhurst tester, brand UWITEC, Austria, for 60 mm internal diameter and 60 cm long PVC crystal tubes, coupled to a 5 m long telescopic aluminum rod (Figure 3), according to the methods described by Abe et al. (2005) and Brasil (2012).

Water samples were collected at 5 and 0.5 cm above the sediment-water interface with the aid of a silicone tube 3 mm in diameter and 60 cm in length, connected to a 20 ml syringe, and transferred to vials glass with silicone septum lids for subsequent CO₂ analysis (Figure 4) (AIIEGA, 2018).

The quantification of CO₂ in the layer above the sediment-water interface was necessary to calculate the

diffusive flow of this gas through the sediment-water interface.

The carbon dioxide diffusive data from this study were collected at 34 georeferenced points on the Teles Pires River, in 4 different campaigns. The database was divided into two levels of reservoir depth, surface, and bottom, of which 25 points were collected on the surface of the reservoir and 9 points on the bottom.

2.4. Statistical analysis of the data

Data were collected over 4 campaigns, which ran from November 2017 to September 2018. The first campaign was carried out in November 2017, which is the flood season for the reservoir. The second in February 2018, when the reservoir is full. The third in June 2018, which is



Figure 3. Photographic record of sediment sample collection in the future reservoir of HPP Sinop with the aid of a telescopic manual rod coupled to the Kajak-Brinkhurst type witness. Source: AIIEGA (2018).



Figure 4. Photographic record of the quantification of temperature and dissolved oxygen (A) and the collection of water samples (B and C) for the quantification of CO_2 in the layer above the sediment-water interface in the sediment core collected in the future reservoir of UHE Sinop. Source: AIIEGA (2018).

the dry season, and the fourth in September 2018, when the reservoir refills.

For the statistical analysis of the data, an exploratory analysis of the data was initially performed, calculating averages, variances, and extreme values of the response variable.

Then, a model was made using the generalized estimation equations of Liang and Zeger (1986).

GHG-based models focus directly on the marginal distribution of the y data, with specification of only the expected value and variance, namely (Equation 1):

$$E(y_{ij}) = \mu_{ij} \quad eV(y_{ij}) = \phi^{-1}\nu(\mu_{ij}) \quad (1)$$

where y_{ij} is the response variable of interest for the j -th individual of the i -th group, $\nu(\mu_{ij})$ is a function of the

expected value and ϕ is the dispersion parameter. The relationship between the expected response and the exploratory variables is specified as Equation 2:

$$g(\mu_{ij}) = X_{ij}^T \beta \quad (2)$$

where g is the link function.

To incorporate the intra-unit sample covariance structure, consider a working covariance matrix defined as Equation 3:

$$\Omega_{W_i}(\theta) = \phi A_i^{1/2} R_W(\theta) A_i^{1/2} \quad (3)$$

where $R_W(\theta)$ is a positive defined matrix of parameters θ . If $R_w(\theta)$ is the true matrix of intra-unit sample correlations of y_i , then $\Omega_{W_i}(\theta) = V(y_i)$.

Due to the continuous nature of the data, a constant was added to make the data positive and thus it was possible to adjust a model using the Gamma distribution considering the identity link function and the depth (surface and bottom) and campaign (1, 2, 3 and 4). Therefore, we have that (Equation 4):

$$\mu^{-1} = \beta_k + \beta_4 X_{ij} \quad (4)$$

where $i = 1, \dots, 34$ refers to the points at which diffusive CO₂ flows were measured, $j = 1, \dots, 4$ to the campaigns in which observations were collected and $k = 1, 2$ at depth (where $k = 1$ surface and $k = 2$ bottom).

The model previously described was tested with the main covariance matrices to choose the covariance matrix that generates the best model for the data.

Pan (2001) proposed a method of selecting a correlation structure for GHG since the measures can be correlated. This criterion was called quasi-likelihood criterion under the independence model (Quasi-Likelihood under the Independence Model Criterion - QIC).

The QIC is calculated by comparing a model with a given work correlation structure with that generated using the independent structure. QIC values can be used to compare different correlation structures. The lower the QIC value, the better the model.

According to the QIC, the correlation matrix chosen was the first order autoregressive, AR(1) (Equation 5). This matrix is used when it is assumed that the measures within the group have a first-order autoregressive relationship, usually when the data are correlated over time. To know,

$$\text{Corr}(y_{ij}, y_{il}) = \theta^{|j-l|}, 1 \leq j, l \leq t_i \quad (5)$$

that is, it is assumed that the correlation between two instants of time decays exponentially according to the distance of the observations.

3. Results

Figure 5 shows the total daily precipitation at the Climatological Station of Sinop-MT (INMET) for the period between November 2017 and September 2018 with an indication of the collection days for the 1st campaign (a), 2nd campaign (b), 3rd field campaign (c) and 4th field campaign (d), carried out by the AIIEGA team in the future reservoir of UHE Sinop.

The rainy season begins most frequently in November and usually extends to March, with the rainiest quarter occurring most frequently between the months of December to March (which may vary from December to February or January to March). The dry season frequently begins in May and generally extends to September, with the peak of the drought in the months of June, July, and August. The month of April acts as a transition from the rainy to the dry season and the month of October makes the transition between the dry and the rainy season (Figure 5).

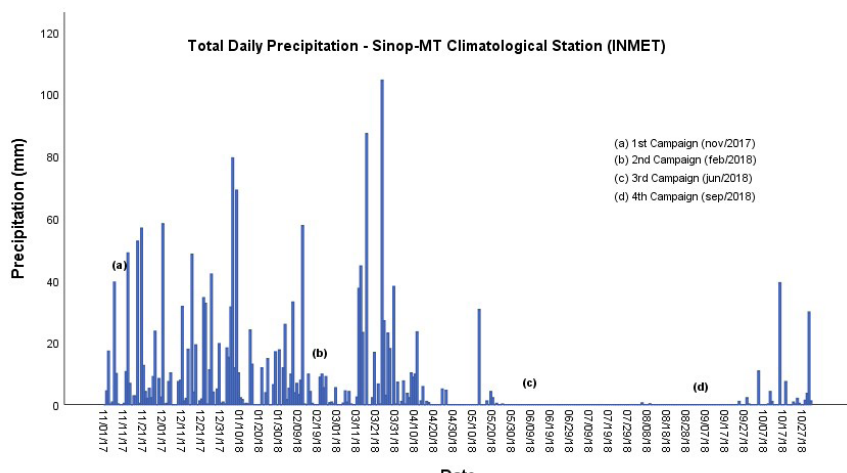


Figure 5. Total daily rainfall at the Sinop-MT Climatological Station (INMET) for the period between November 2017 and September 2018. Source: Agritempo (2018).

An exploratory analysis of the data was carried out, and in general, the diffusive CO₂ emission was 2,934.97 mg.m⁻².d⁻¹.

The highest value for emissions was 10,112.80 mg.m⁻².d⁻¹ as well as the highest average 6,030.77 mg.m⁻².d⁻¹ was measured on the surface of the reservoir in the 2nd campaign, which is equivalent to the rainy season in the reservoir. In July and September 2018, negative values were measured on the surface of the reservoir, which indicates absorption of gas by the reservoir (Table 1).

The values for the measurements of the diffusive flow of CO₂ seem more variable on the surface of the reservoir throughout the campaigns, while in the end the emissions seem to have a more similar behavior. This behavior can be seen in the scatter plot in Figure 6.

To have a general illustration of each depth level of the reservoir, the graph of Figure 7 shows the average diffusive emission of CO₂ for the surface and bottom, and the variation of the average emission interval of each level and its evolution over the four campaigns.

The average profile per campaign, defined as the average diffusive CO₂ emission per campaign by depth, shows a growth from campaign 1 to campaign 2 both on the surface and at the bottom, then shows a decay from campaign 2 to 3 and to surface, there is a slight growth from campaign 3 to campaign 4.

Through Wald's chi-square test (Table 2), it is noted that the data have a p-value well below 0.01, that is, there is an effect of depth and of the campaign on diffusive CO₂ emissions, that is, there is an influence of when emissions were collected and whether they were collected on the surface or bottom of the reservoir.

This means that emissions are different when measured on the surface and bottom of the reservoir, and that they also vary over time.

It is also possible to see that there is an effect of the interaction (depth x campaign), this result shows that during the campaigns there is a change in the average behavior of diffusive CO₂ emissions between the levels of the reservoir.

Table 1. Descriptive statistics of CO₂ diffusive flow measurements by campaign and depth.

Campaign	Depth	Minimum	Maximum	Average	Median	Standard Deviation
Nov/2017	Bottom	565.51	2,275.75	1,170.65	1,062.03	545.15
	Surface	577.21	8,549.25	3,760.98	3,422.21	2,402.62
Feb/2018	Bottom	530.88	4,146.25	1,868.67	1,980.34	1,142.96
	Surface	1,766.10	10,112.80	6,030.77	6,465.50	2,392.23
Jun/2018	Bottom	530.61	3,719.55	1,501.85	1,063.31	1,009.34
	Surface	-1,447.10	6,757.50	1,892.16	1,932.65	2,115.64
Sep/2018	Bottom	484.02	3,971.52	1,310.38	978.21	1,081.99
	Surface	-3,025.10	6,213.70	2,096.55	1,862.70	1,963.55

Source: Own elaboration.

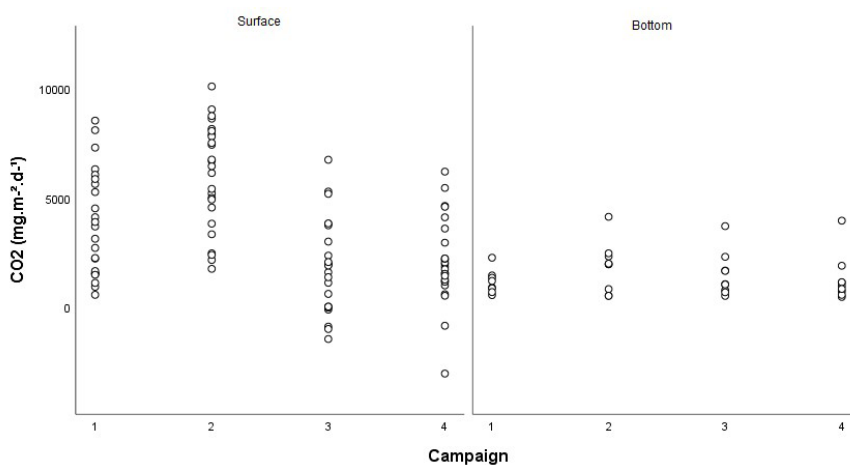


Figure 6. Scatter plot for diffusive CO₂ emissions per campaign separated by depth. Source: Own elaboration.

Table 3 shows the results of the average diffusive CO₂ emissions, the standard error, and the confidence intervals for each level of the reservoir in each campaign.

Note that the averages of CO₂ diffusive emissions on the reservoir surface are higher in campaigns 1 and 2 than in campaigns 3 and 4, as well as higher than the averages observed at the bottom of the reservoir for all campaigns. For the bottom of the reservoir, the averages of the diffusive emissions of carbon dioxide are very similar between the campaigns.

One of the most important steps in any modeling process is the diagnostic analysis, through which possible deviations from the assumptions made by the model are verified, in addition to allowing to find possible extreme observations that disproportionately interfere with the results of the adjustment.

The diagnostic analysis started with the analysis of residues to verify possible observations that present a great distance from the others (outliers), a point that exert a disproportionate weight in the estimates of the model parameters (influential observations) or to evaluate the adequacy of the distribution proposed for the response variable.

The method of local influence proposed by Cook (1986) consists of verifying, through an appropriate measure of influence, the robustness of the estimates provided by the model in the face of the effect of small disturbances in the model itself or data.

Table 2. Results of the test of the main effects and of the interaction by Wald's chi-square.

	Wald's chi-square	Degrees of freedom	p-Value (Wald)
(Intercept)	1,630.64	1	0.00
Depth	45.98	1	0.00
Campaign	46.67	3	0.00
Depth * Campaign	32.91	3	0.00

Source: Own elaboration.

Table 3. Estimates of the average diffusive CO₂ emissions by depth and campaign.

Depth Campaign		Average	Standard Error	95% Wald Confidence Interval	
				Lower	Higher
Bottom	1	4,638.39	176.77	4,304.56	4,998.12
	2	5,368.67	359.20	4,708.86	6,120.93
	3	5,001.85	317.20	4,417.22	5,663.85
	4	4,810.38	340.04	4,188.03	5,525.21
Surface	1	7,271.00	480.50	6,387.69	8,276.47
	2	9,530.77	468.78	8,654.87	10,495.30
	3	5,420.82	421.61	4,654.39	6,313.46
	4	5,596.55	384.78	4,891.00	6,403.87

Source: Own elaboration.

Figure 8 shows the graph of Cook's distance indices for the model adjusted to the diffusive CO₂ emissions data.

By Figure 8, it is possible to notice that there are some observations that are more distant from the majority, but do not present great highlights, therefore, there are no observations causing disturbances in the model.

To prove the adequacy of the adjusted model, the Shapiro-Wilk normality test was performed with the residues of the model. The p-value of the test was 0.225, which accepts the null hypothesis that the data follow a normal distribution. Figure 9 shows the Q-Qplot of the residues and the data are all close to the line, which proves normality.

4. Discussion

Through a complementary test, it is possible to assess where the change in the average behavior of diffuse carbon dioxide emissions occurs. The post-hoc test performed was the Bonferroni test, this test makes peer-to-peer comparisons between the campaigns and the depth to detect where the effect found in the test in Table 2 exists and thus decrease the chance of type I error.

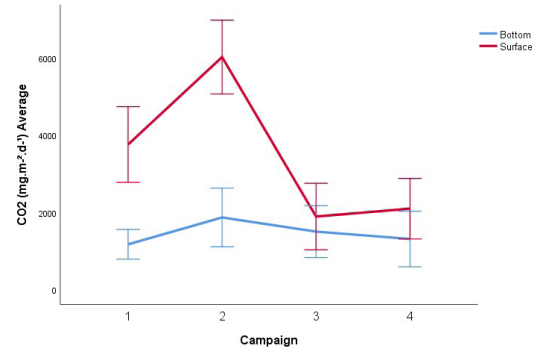


Figure 7. Average profile of diffusive CO₂ emissions at each level throughout the campaigns. Source: Own elaboration.

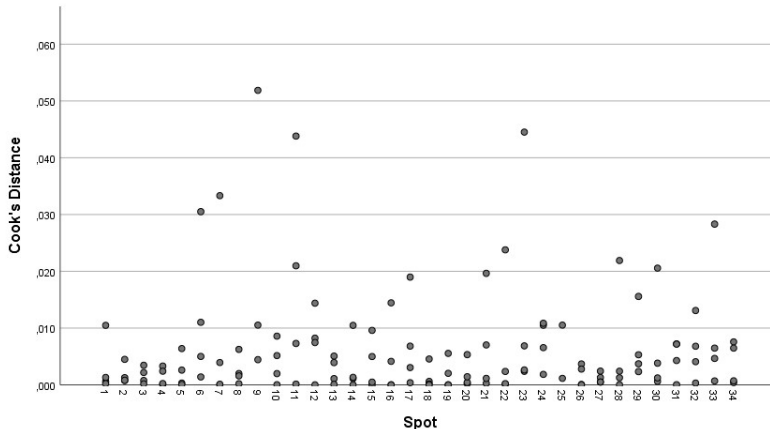


Figure 8. Graph of the approximate Cook's distance, referring to the gamma model adjusted to the data on diffusive CO₂ emissions.
Source: Own elaboration.

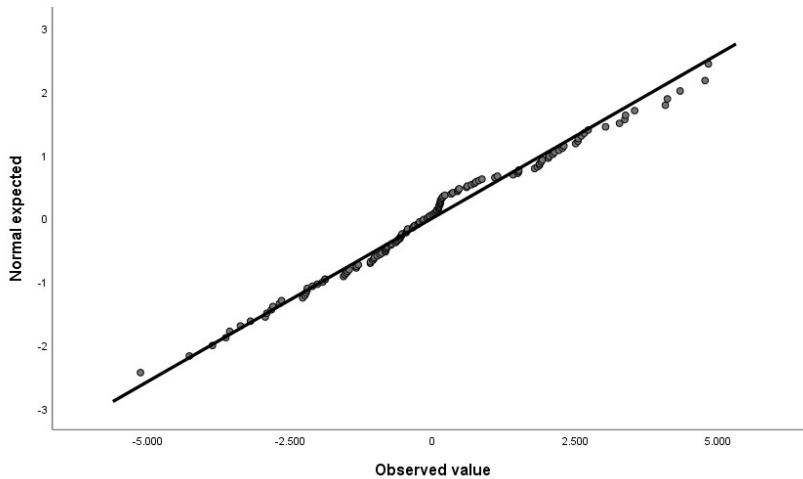


Figure 9. Q-Qplot of the residuals of the adjusted model for diffusive CO₂ emissions. Source: Own elaboration.

Tables 4 and 5 show the peer-to-peer comparisons of the interaction effect. Table 4 fixes the campaign and compares the depths, different from Table 5, which fixes the depth and compares the campaigns.

From the results of Table 4, it can be noted that there is a difference in diffusive CO₂ emissions between surface and bottom only in campaigns 1 and 2 (*p*-value < 0.05). In campaign 1, the average of emissions was higher on the surface (*p*-value < 0.001). The same result occurs in campaign 2, which corroborates the results described in Table 3.

It is also noted that emissions on the surface are higher than those in the bottom in all campaigns, which can be explained by the production of carbon dioxide in the water column by the breathing process of aquatic organisms (Rogerio et al., 2013; Lu et al., 2020).

In 2011 and 2012, Marcelino et al. (2015) measured diffusive CO₂ emissions in Serra da Mesa and the study

found no statistically significant differences between the rainy (January) and dry (July) seasons, however, it found differences between the wet to dry transition periods (April) and dry to wet (October).

In Table 5, significant difference (*p*-value < 0.05) was found between campaign 1 and 2, and between campaigns 2 and 3, with a higher mean for campaign 2, both cases presented on the surface reservoir.

This information can be justified by the rainy season in the reservoir region, as campaign 2 (February) is equivalent to the rainy and flood season of the reservoir while campaign 3 (June) is the time of the drought peak.

For the bottom of the reservoir, there was only a significant difference in diffusive CO₂ emissions only between campaigns 1 and 2, with a higher average emission in campaign 2. There are no differences between campaigns 3 and 4.

Table 4. Partial results of multiple comparisons of the interaction effect (depth * campaign) on the diffusive CO₂ emission variable fixing the campaign.

Campaign	Depth (i)	Depth (j)	Mean Difference (i-j)	Standard Error	Degrees of freedom	p-Value (Bonferroni)	95% Wald Confidence Interval	
							Lower	Higher
1	Bottom	Surface	-2,632.61	511.98	1	0.00	-3,636.07	-1,629.15
	Surface	Bottom	2,632.61	511.98	1	0.00	1,629.15	3,636.07
2	Bottom	Surface	-4,162.10	590.57	1	0.00	-5,319.61	-3,004.60
	Surface	Bottom	4,162.10	590.57	1	0.00	3,004.60	5,319.61
3	Bottom	Surface	-418.97	527.61	1	0.43	-1,453.06	615.12
	Surface	Bottom	418.97	527.61	1	0.43	-615.12	1,453.06
4	Bottom	Surface	-786.17	513.49	1	0.13	-1,792.60	220.26
	Surface	Bottom	786.17	513.49	1	0.13	-220.26	1,792.60

Source: Own elaboration.

Table 5. Partial results of multiple comparisons of the interaction effect (depth * campaign) on the diffusive CO₂ emission variable, setting the depth.

Depth	Campaign (i)	Campaign (j)	Mean Difference (i-j)	Standard Error	Degrees of freedom	p-Value (Bonferroni)	95% Wald Confidence Interval	
							Lower	Superior
Bottom	1	2	-730.27	250.31	1	0.02	-1,390.66	-69.89
		3	-363.45	395.82	1	1.00	-1,407.73	680.82
		4	-171.99	412.44	1	1.00	-1,260.11	916.14
	2	1	730.27	250.31	1	0.02	69.89	1,390.66
		3	366.82	463.03	1	1.00	-854.76	1,588.41
		4	558.29	608.29	1	1.00	-1,046.53	2,163.10
	3	1	363.45	395.82	1	1.00	-680.82	1,407.73
		2	-366.82	463.03	1	1.00	-1,588.41	854.76
		4	191.46	566.78	1	1.00	-1,303.84	1,686.77
	4	1	171.99	412.44	1	1.00	-916.14	1,260.11
		2	-558.29	608.29	1	1.00	-2,163.10	1,046.53
		3	-191.46	566.78	1	1.00	-1,686.77	1,303.84
Surface	1	2	-2,259.77	700.06	1	0.01	-4,106.70	-412.83
		3	1,850.19	609.04	1	0.01	243.38	3,456.99
		4	1,674.46	558.07	1	0.02	202.11	3,146.80
	2	1	2,259.77	700.06	1	0.01	412.83	4,106.70
		3	4,109.95	519.90	1	0.00	2,738.31	5,481.59
		4	3,934.22	541.02	1	0.00	2,506.87	5,361.57
	3	1	-1,850.19	609.04	1	0.01	-3,456.99	-243.38
		2	-4,109.95	519.90	1	0.00	-5,481.59	-2,738.31
		4	-175.73	435.33	1	1.00	-1,324.24	972.78
	4	1	-1,674.46	558.07	1	0.02	-3,146.80	-202.11
		2	-3,934.22	541.02	1	0.00	-5,361.57	-2,506.87
		3	175.73	435.33	1	1.00	-972.78	1,324.24

Source: Own elaboration.

5. Conclusions

The adjusted GHG model allowed the analysis of diffusive CO₂ emissions between the reservoir, surface, and bottom levels and throughout the campaigns. A statistically significant difference was found in the average emissions both between the depth levels of the future reservoir and throughout the campaigns.

It was noted that the average diffusive CO₂ emissions are higher when collected on the surface of the reservoir than on the bottom.

It was also detected that the average of emissions is higher during campaign 2 (February 2018), which is equivalent to the rainy season in the reservoir region, a fact that corroborates the descriptive analyzes carried out initially.

Therefore, the study showed that the period of rain and drought influence the diffusive emissions of CO₂ as well as the depth at which the data are collected, considering that according to the precipitation the fluvimetric station of the reservoir is changed.

The longitudinal study allowed the creation of a regression model that explained the behavior of diffusive CO₂ emissions over time and within the future reservoir. This allows the researcher a sense of the environment in which the data is collected and the influence they may be subjected to.

Acknowledgements

We thank SINOP energy for the opportunity to work with data from hydroelectric plants in Brazil and CNPq for the doctoral scholarship of the first author that contributed to the development of this study and the second author for science productivity scholarship. We thank also to the AIIEGA/São Carlos to permit the use of bottom diffusion flux data.

References

- ABE, D.S., ADAMS, D.D., SIDAGIS-GALLI, C., SIKAR, E. and TUNDISI, J.G., 2005. Sediment greenhouse gases (methane and carbon dioxide) in the Lobo-Broa Reservoir, São Paulo State, Brazil: concentrations and diffuse emission fluxes for carbon budget considerations. *Lakes and Reservoirs*, vol. 10, no. 4, pp. 201-209. <http://dx.doi.org/10.1111/j.1440-1770.2005.00277.x>.
- ABRIL, G., GUÉRIN, F., RICHARD, S., DELMAS, R., GALY-LACAUX, C., GOSSE, P., TREMBLAY, A., VARFALVY, L., SANTOS, M.A. and MATVIENKO, B., 2005. Carbon dioxide and methane emissions and the carbon budget of a 10-years old tropical reservoir. (Petit-Saut, French Guiana). *Global Biogeochemical Cycles*, vol. 19, no. 4, pp. 1-16. <http://dx.doi.org/10.1029/2005GB002457>.
- ASSOCIAÇÃO INSTITUTO INTERNACIONAL DE ECOLOGIA E GERENCIAMENTO AMBIENTAL – AIIEGA, 2018. *Relatório Final Consolidado do Projeto de Estudo “Monitoramento de Fluxos de Gases de Efeito Estufa e de Parâmetros de Qualidade da Água na Área da UHE Sinop”*. Relatório Interno. São Carlos, 67 p.
- BARBOSA, P.M., FARJALLA, V.F., MELACK, J.M., AMARAL, J., DA SILVA, J. and FORSBERG, B., 2018. High rates of methane oxidation in an Amazon floodplain lake. *Biogeochemistry*, vol. 137, no. 3, pp. 351-365. <http://dx.doi.org/10.1007/s10533-018-0425-2>.
- BORGES, A.V., DELILLE, B., SCHIETTECATTE, L.S., GAZEAU, F., ABRIL, G. and FRANKIGNOULLE, M., 2004. Gas transfer velocities of CO₂ in three European estuaries (Randers Fjord, Scheldt and Thames). *Limnology and Oceanography*, vol. 49, no. 5, pp. 1630-1641. <http://dx.doi.org/10.4319/lo.2004.49.5.1630>.
- BRASIL. Ministério de Minas e Energia – MME, 2012. *Diretrizes para análises quantitativas de emissões líquidas de gases de efeito estufa em reservatórios. Programas de medição e análise de dados*. Rio de Janeiro: MME, vol. 1, 95 p.
- BRASIL, 2020 [viewed 14 January 2021]. *Fontes de energia renováveis representam 83% da matriz elétrica brasileira* [online]. Available from: <https://www.gov.br/pt-br/noticias/energia-minerais-e-combustiveis/2020/01/fontes-de-energia-renovaveis-representam-83-da-matriz-eletrica-brasileira>
- CHEN, Z., YE, X. and HUANG, P., 2018. Estimating carbon dioxide (CO₂). *Emissions from Reservoirs Using Artificial Neural Networks*, vol. 10, pp. 26.
- COOK, R.D., 1986. Assessment of local influence. *Journal of the Royal Statistical Society. Series B. Methodological*, vol. 48, no. 2, pp. 133-155. <http://dx.doi.org/10.1111/j.2517-6161.1986.tb01398.x>.
- DAMAZIO, J.M., SANTOS, M.A., XAVIER, V.L., MEDEIROS, A.M., MARCELINO, A.A., AMORIM, M.A., BEZERRA, C.S., ROGERIO, J.P., SIKAR, D.M., SIKAR, E.M. and MATVIENKO, B., 2013. Uso da mediana para estimativa robusta de taxa de emissão difusiva de gases de efeito estufa em reservatórios a partir de medições pontuais com câmaras flutuantes espacialmente distribuídas. In: *XX Simpósio Brasileiro de Recursos Hídricos*, 2013, Bento Gonçalves. Porto Alegre: Associação Brasileira de Recursos Hídricos.
- GOLBI, M.F., 2015. *Introdução à modelagem da poluição ambiental*. Curitiba: Universidade Federal do Paraná.
- GUÉRIN, F., ABRIL, G., SERÇA, D., DELON, C., RICHARD, S., DELMAS, R., TREMBLAY, A. and VARFALVY, L., 2007. Gas transfer velocities of CO₂ and CH₄ in a tropical reservoir and its river downstream. *Journal of Marine Systems*, vol. 66, no. 1-4, pp. 161-172. <http://dx.doi.org/10.1016/j.jmarsys.2006.03.019>.
- INSTITUTO ALBERTO LUIZ E COIMBRA DE PÓS-GRADUAÇÃO E PESQUISA EM ENGENHARIA – COPPE, 2018. *Relatório de Medições 4ª Campanha do Estudo “Monitoramento de Fluxos de Gases de Efeito Estufa e de Parâmetros de Qualidade da Água na Área da UHE Sinop*. Relatório Interno. Rio de Janeiro, 93 p.
- INTERNATIONAL HYDROPOWER ASSOCIATION – IHA, 2010. *GHG measurement guidelines for freshwater reservoirs*. London: IHA, 138 p.
- LIANG, K.-Y. and ZEGER, S.L., 1986. Longitudinal data analysis using generalized linear models. *Biometrika Trust*, vol. 73, no. 1, pp. 13-22. <http://dx.doi.org/10.1093/biomet/73.1.13>.
- LU, S., DAI, W., TANG, Y. and GUO, M., 2020. A review of the impact of hydropower reservoirs on global climate change. *The Science of the Total Environment*, vol. 711, pp. 134996. <http://dx.doi.org/10.1016/j.scitotenv.2019.134996>. PMid:31818589.
- MARCELINO, A.A., SANTOS, M.A., XAVIER, V.L., BEZERRA, C.S., SILVA, C.R.O., AMORIM, M.A., RODRIGUES, R.P. and ROGERIO, J.P., 2015. Diffusive emission of methane and carbon dioxide from two hydropower reservoirs in Brazil. *Brazilian Journal of Biology = Revista Brasileira de Biologia*, vol. 75, no. 2, pp. 331-338. <http://dx.doi.org/10.1590/1519-6984.12313>. PMid:26132015.
- MERCADO BURCIAGA, U., SÁEZ, P. and HERNÁNDEZ AYÓN, F., 2019. Strategies to reduce CO₂ emissions in housing building by means of CDW. *Emerging Science Journal*, vol. 3, no. 5, pp. 274-284. <http://dx.doi.org/10.28991/esj-2019-01190>.

- NELDER, J.A. and WEDDERBURN, R.W.M., 1972. Generalized linear models. *Journal of the Royal Statistical Society A*, vol. 135, no. 3, pp. 370-384. <http://dx.doi.org/10.2307/2344614>.
- NOBRE, J.S. and SINGER, J.M., 2007. Residual analysis for linear mixed models -. *Biometrical Journal. Biometrische Zeitschrift*, vol. 49, no. 6, pp. 863-875. <http://dx.doi.org/10.1002/bimj.200610341>. PMid:17638292.
- PAN, W., 2001. Akaike's information criterion in generalized estimating equations. *Biometrics*, vol. 57, no. 1, pp. 120-125. <http://dx.doi.org/10.1111/j.0006-341X.2001.00120.x>. PMid:11252586.
- ROGÉRIO, J.P., SANTOS, M.A. and SANTOS, E.O., 2013. Influence of environmental variables on diffusive greenhouse gas fluxes at hydroelectric reservoirs in Brazil. *Brazilian Journal of Biology* = *Revista Brasileira de Biologia*, vol. 73, no. 4, pp. 753-764. <http://dx.doi.org/10.1590/S1519-69842013000400011>. PMid:24789391.
- SHERMAN, G.E., SUTTON, T., BLAZEK, R., HOLL, S., DASSAU, O., MORLEY, B., MITCHELL, T. and LUTHMAN, L., 2011 [viewed 5 November 2018]. *Quantum GIS user guide - Version 1.7 "Wroclaw"* [online]. Available from: http://download.osgeo.org/qgis/doc/manual/qgis1.7.0_user_guide_en.pdf
- SINOP ENERGIA [online], 2021 [viewed 14 January 2021]. Available from: <https://www.sinopenergia.com.br>
- SISTEMA DE MONITORAMENTO AGROMETEOROLÓGICO – AGRITEMPO, 2018 [viewed 5 November 2018]. *Banco de dados meteorológicos de Mato Grosso* [online]. Available from: <https://www.agritempo.gov.br/agritempo/jsp/PesquisaClima/index.jsp?siglaUF=MT>